Vibrational fine structures revealed by the real-time vibrational phase and amplitude in MEH-PPV using few cycle pulses

Jun Zhang,[1] Zhuan Wang,[1,2] and Takayoshi Kobayashi[1,2,3,4]

[1]*Department of Applied Physics and Chemistry and Institute for Laser Science, The University of Electro-Communications, 1-5-1 Chofugaoka, Chofu, Tokyo 182-8585, Japan*

[2]*Ultrashort Pulse Laser Project, ICORP, JST, 4-1-8 Honcho, Kawaguchi, Saitama 332-0012, Japan*

[3]*Department of Electrophysics, National Chiao Tung University, 1001 Ta Hsueh Road, Hsin-Chu 3005, Taiwan*

[4]*Institute of Laser Engineering, Osaka University, 2-6 Yamada-Oka, Suita, Osaka 565-0971, Japan*

It was found that the vibronic transition peaks hidden in a featureless spectrum of induced absorption could be clearly revealed by utilizing the spectra of phases and amplitudes of the molecular vibrational modes. Some of the peaks were also found in a second derivative of a transition spectrum integrated over a delay time from 100 to 700 fs. This is because of the localization of a wave packet in a limited region along the potential multimode hypersurfaces. The transition energy of an induced absorption or an induced emission corresponds to some localized point (space) on the potential hypersurface to which the wave packets visit with some fixed phases.

PACS number(s): 78.47.−p, 33.70.Ca, 36.20.Ng

Properties such as the plasticity, chemical modification capability, and semiconductivity[1–4] make conjugated polymers remarkably excellent candidates for electro-optical device applications. Therefore, research activities on the efficiency and the dynamics of elementary excitations in conjugated polymers have recently been stimulated by the potential application in optoelectronic devices.[5–8] In particular, considerable progress has been made in the development of electroluminescent devices based on poly(arylenevinylene)s in recent years.[9,10] One of the most important and extensively studied conjugated polymers is poly-[2-methoxy, (5-2′-ethyl-hexyloxy)-*p*-phenylenevinylene] (MEH-PPV) because of its high electroluminescence quantum efficiency and solubility in common solvents.

Through the extensive study of the mechanism of a luminescence process in MEH-PPV, it was found that it could be described in terms of an exciton.[11–13] A detailed understanding of the dynamics of photoexcitations in MEH-PPV is highly desirable for practical reasons because they are related to the radiationless relaxation, which determines luminescence efficiency. In order to clarify the mechanism of the fast radiationless decay dynamics, it is most straightforward to utilize pulse lasers in transient nonlinear spectroscopy techniques such as absorption, gain, grating, and stimulated Raman scattering.[14–16] When ultrafast pulse duration is shorter than molecular vibrational periods, the vibrational dynamics can also be studied as described in previous papers.[17–19]

Pulse lasers with pulse durations of several tens to hundreds of femtoseconds were used to study MEH-PPV.[20–22] However, no study has been reported on the coherent molecular vibration induced by an impulsive excitation using a short enough pulse to excite coherent vibration.

In this Brief Report, the dependence of vibrational amplitude on probe photon energy is discussed for the wavelength range, where the intensity of ground-state absorption is negligibly small. From this, a vibrational spectroscopic structure hidden in a broad induced absorption spectrum could be revealed by the phase information of the molecular vibration.

This phase information cannot be obtained by conventional time-resolved (TR) vibrational spectroscopies such as TR, IR absorption, and TR Raman scattering.

A noncollinear optical parametric amplifier[23–25] (NOPA) was used as a light source of the pump-probe experiment, as described in our previous papers.[17–19] Several features of the system are described below. The pump source of this system is a commercially supplied regenerative amplifier (Spectra Physics, Spitfire). Its central wavelength, pulse duration, repetition rate, and average output power were 790 nm, 50 fs, 5 kHz, and 800 mW, respectively. The output pulse from the NOPA was compressed with a compressor composed of a pair of prisms and chirp mirrors. The pulse duration was 5.7 fs and covered the spectral range from 520 to 750 nm. The pulse energies of the pump and probe were about 35 and 5 nJ, respectively. A 128-channel lock-in amplifier was used as a phase-sensitive broadband detector.[19] Chloroform solutions of MEH-PPV were spin-coated onto quartz plates to form $0.5–1.0$ μm thick films. All the experiments were performed at room temperature (293 ± 1 K).

The pump-probe experiment of a MEH-PPV sample film was performed with a probe delay time from −200 to 1800 fs. The absorbance change induced by the pump is probed as a function of probe delay time. The curve of the absorbance change versus probe delay time is called real-time (vibration) trace or vibration real-time spectrum.

Figures 1(a) and 1(b) show the real-time traces and fast Fourier-transform (FFT) power spectra of the traces calculated for the time range from 50 to 1800 fs, respectively, at ten typical, different wavelengths. The time range between 0 and 50 fs was not used for the FFT calculation to avoid the interference between the scattered pump and probe pulses.

In the power spectra shown in Fig. 1(b), there are several intense peaks at 961, 1278, 1315, and 1587 cm^{-1}. In order to clarify the mechanism of the modulation of transition probability due to the molecular vibration, the probe photon energy dependence of the vibrational amplitude and phase are shown in Fig. 2. Among all of the modes, there are intense
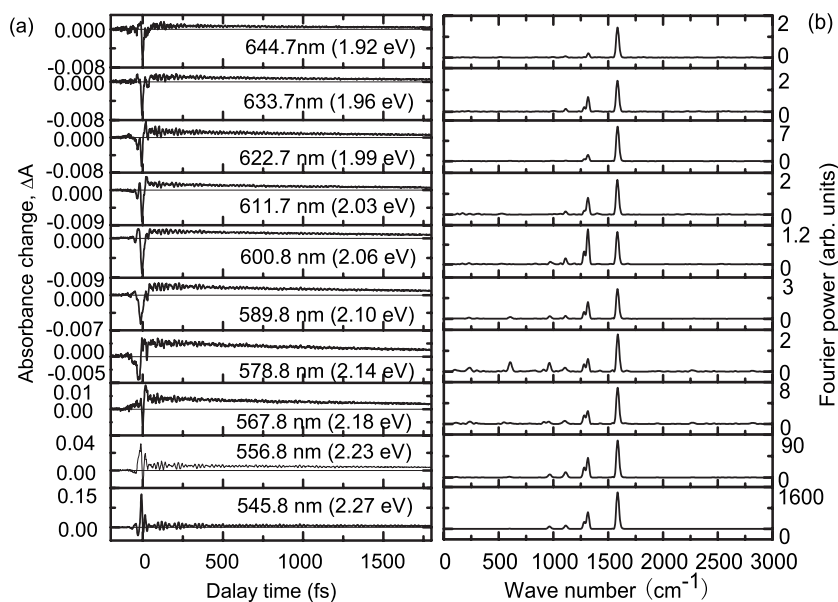
FIG. 1. Real-time vibrational spectra and FFT power spectra of molecular vibration at ten different probe wavelengths. (a) The change in the absorbance as a function of pump-probe delay time at various probe photon energies. (b) The FFT power spectra of real-time vibrational spectra at the corresponding probe photon energies.

amplitude ranges in the probe photon energy higher than 2.2 eV. In our previous paper, the intense amplitude range extending in the ground-state absorption spectral region was studied in detail and was explained in terms of the ground-state wave packet induced by the time-dependent Franck–Condon (FC) effect and non-Condon (NC) effect.[26,27] FC and NC contribute to the spectral dependence described by the first derivative and the zeroth and second derivatives, respectively, of the ground-state absorption spectrum.

Here, in this Brief Report, we would like to discuss in detail the probe photon energy dependence of the vibrational amplitude of the most intense modes with frequencies of 1278, 1315, and 1587 cm^{-1} in the spectral range below the absorption edge.

Figures 2(a)–2(c) show the probe photon energy (wavelength) dependence of vibrational phases and amplitudes of the vibrational modes with frequencies of 1587, 1315, and 1278 cm^{-1}, respectively. It can be found in Fig. 2(a) that the amplitude and phase spectra have a distinct structure, with the peaks and valleys at nearly the same photon energies. Similar features also exist in Figs. 2(b) and 2(c). Table I lists these extrema appearing in the amplitude and phase spectra corresponding to modes of 1587, 1315, and 1278 cm^{-1}, as shown in Fig. 2. The probe photon energy corresponding to the distance between the neighboring peaks and valleys are nearly equal. This means that these extrema can correspond to the peaks and/or valleys forming a vibrational progression in the time-resolved spectrum. Peaks may correspond to the excited state absorption peaks, and valleys may correspond to the peaks of induced emission. In the latter case, a negative absorbance due to a bleaching induced by a ground-state depletion can be neglected because of the absence of a sufficiently intense fluorescence in this range.

Figure 3 shows the time-resolved absorption spectra of the sample integrated over the delay time ranging from 100 to 700 fs and its first and second derivatives with respect to photon energy. It can be observed that the time-resolved spectrum does not have a clear structure due to either a vibrational progression or other electronic states. However, it

is known that a faint feature in the spectrum can be resolved by calculating its second derivative. The peak of the second derivative can either be the peak or valley hidden in the original (zeroth derivative) spectrum. Therefore, it can be found in Fig. 3 that the second derivative calculated for the delay time integrated time-resolved spectrum has a fine structure composed of several peaks and valleys. These extrema (peaks and valleys) are also listed in Table I.
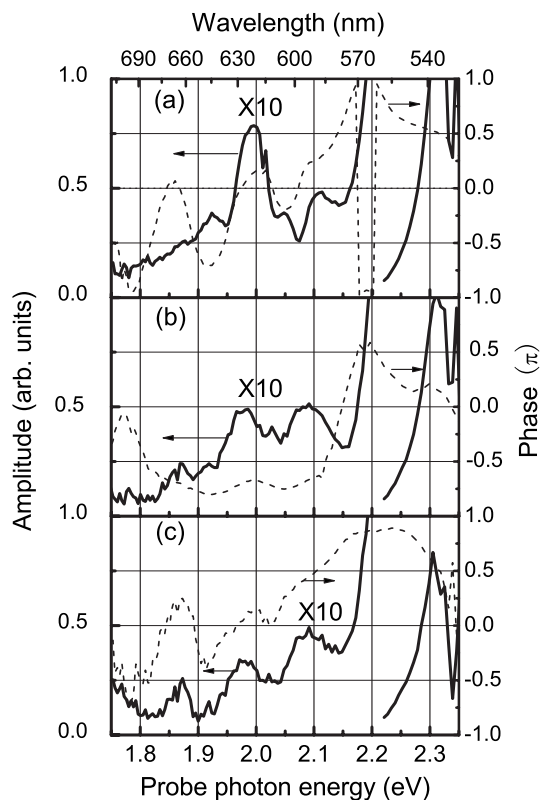

FIG. 2. FFT amplitude (solid curve; the part of the photon energy smaller than 2.21 eV is magnified ten times for details) and phase (dashed curve) corresponding to the modes (a) 1587 cm^{-1}, (b) 1315 cm^{-1}, and (c) 1278 cm^{-1}, respectively.

TABLE I. The extrema of the second derivatives (2ndD) of the integrated time-resolved spectrum with respect to the probe delay time over 100–700 fs, the vibrational phase (Φ) with respect to the zero probe delay time, and the amplitude (A) of the molecular vibrations corresponding to the modes of 1587, 1315, and 1278 cm^{-1}, respectively.

Mode (cm^{-1})	2ndD extrema (eV)	Φ extrema (eV)	A extrema (eV)
1587	1.82	1.86	
	1.91	1.92	
	2.00	2.01	1.99
		2.05	2.05
	2.12		2.11
1315	1.82		1.88
	1.91	1.92	
	2.00	2.00	1.98
		2.05	2.04
	2.12		2.15
1278	1.82	1.87	1.87
	1.91	1.92	1.91
	2.00	2.00	1.98
		2.02	2.03
			2.09
	2.12		2.14

From Table I, there are extrema (peaks and valleys) commonly found in the second derivative of the transient absorption spectrum ($d^2A/d\omega^2$), and phase (Φ) and amplitude (A) spectra of the molecular vibration. For the 1587 cm^{-1} mode, there are four extrema in the second derivative of the time-resolved absorption spectrum. They are located at 1.82, 1.91, 2.00, and 2.12 eV. These highest energy peaks appear within the vicinity of 0.04 eV of the three relevant extrema. The phase and amplitude spectra have common extrema at around 2.00 and 2.05 eV. The former also exists in the second derivative. In the case of the 1315 and 1278 cm^{-1} modes, the extremum near 2.00 eV exists in all of the spectra of the second derivative, the phase, and the amplitude. There are four common extrema among those of the second derivative, phase (Φ), and amplitude (A) spectra for the 1278 cm^{-1} mode.

The extrema found in the second derivative have equal distances of about 0.09 eV. This may be related to the peaks in the integrated absorption spectra shown in Fig. 3, which may contain a vibrational progression of 1440 cm^{-1} corre-
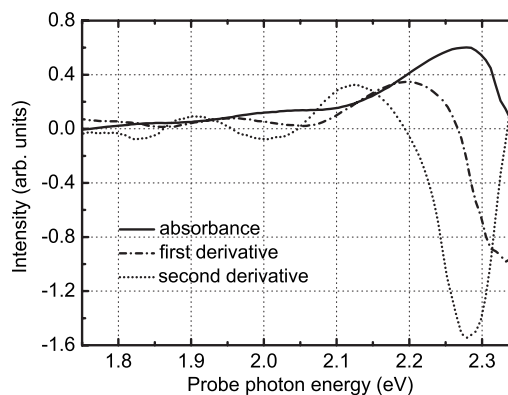

FIG. 3. Absorbance change (solid curve), its first derivative (dash-dotted curve), and second derivative (dotted curve).

sponding to 0.18 eV, which is twice the value of 0.09 eV. Further study is in progress to analyze the absorption phase of the vibrational modes to clarify the origin of these peaks. The exact assignment of these peaks is not easy at present, but they are considered to be vibronic transitions not clearly detected in the time-resolved spectra. Some of them could actually be found in the time-resolved spectra by utilizing the second derivative.

In conclusion, we could find the vibronic structure and progression hidden in the featureless spectrum of an induced absorption by utilizing the spectra of phases and amplitudes of the molecular vibrational modes. This appears because of the localization of the wave packet along the potential multimode hypersurfaces. The transition energy of the induced absorption or induced emission corresponds to some localized point (space) on the hypersurface, to which the wave packets visit with some fixed phases. The method complements the second derivative method of a transient absorption spectrum. By utilizing the data taken by this method, the structure of potential hypersurfaces may be constructed by a detailed analysis of the time-resolved spectrum and the spectra of phase and amplitude of various vibrational modes appearing in the Fourier power spectra of real-time traces.

[1] L. J. Rothberg and A. J. Lovinger, J. Mater. Res. **11**, 3174 (1996).

[2] F. Hide, M. A. Díaz-García, B. J. Schwartz, and A. J. Heeger, Acc. Chem. Res. **30**, 430 (1997).

[3] R. H. Friend, R. W. Gymer, A. B. Holmes, J. H. Burroughes, R. N. Marks, C. Talian, D. D. C. Bradley, D. A. dos Santos, J. L. Brédasa, M. Lodlung, and W. R. Salaneck, Nature (London) **397**, 121 (1999).

[4] G. A. M. Sáfar, F. A. C. Oliveira, L. A. Cury, A. Righi, P. L. M. Barbosa, P. Dieudonné, and F. S. Lameiras, J. Appl. Polym. Sci. **102**, 5620 (2006).

[5] T. Kobayashi, *Nonlinear Optics of Organics and Semiconductors*

(Springer, Berlin, 1989).

[6] S. Etemad and Z. G. Soos, in *Spectroscopy of Advanced Materials*, edited by R. J. H. Clark and R. E. Hester (Wiley, New York, 1991).

[7] R. F. Mahrt, T. Pauck, U. Lemmer, U. Siegner, M. Hopmeier, R. Hennig, H. Bässler, E. O. Göbel, P. Haring Bolivar, G. Wegmann, H. Kurz, U. Scherf, and K. Mullen, Phys. Rev. B **54**, 1759 (1996).

[8] A. J. Heeger, S. Kivelson, J. R. Schrieffer, and W.-P. Su, Rev. Mod. Phys. **60**, 781 (1988).

[9] P. L. Burn, A. B. Holmes, A. Kraft, D. D. C. Bradley, A. R. Brown, R. H. Friend, and R. W. Gymer, Nature (London) **356**, 47 (1992).

[10] G. R. Hayes, I. D. W. Samuel, and R. T. Phillips, Phys. Rev. B **52**, R11569 (1995).

[11] M. Liess, S. Jeglinski, Z. V. Vardeny, M. Ozaki, K. Yoshino, Y. Ding, and T. Barton, Phys. Rev. B **56**, 15712 (1997).

[12] S. Abe, J. Phys. Soc. Jpn. **58**, 62 (1989).

[13] T. Ogawa and T. Takagahara, Phys. Rev. B **44**, 8138 (1991).

[14] *Femtochemistry*, edited by F. C. Schryver, S. Feyter, and G. Schweitzer (Wiley-VCH, Weinheim, Germany, 2001).

[15] *Femtochemistry and Femtobiology*, edited by A. Douhal and J. Santamaria (World Scientific, Singapore, 2001).

[16] *Femtochemistry VII Fundamental Ultrafast Processes in Chemistry, Physics, and Biology*, edited by A. W. Castleman, Jr. and M. L. Kimble (Elsevier, The Netherlands, 2006).

[17] T. Kobayashi, T. Saito, and H. Ohtani, Nature (London) **414**, 531 (2001).

[18] T. Kobayashi, A. Shirakawa, H. Matsuzawa, and H. Nakanishi, Chem. Phys. Lett. **321**, 385 (2000).

[19] N. Ishii, E. Tokunaga, S. Adachi, T. Kimura, H. Matsuda, and T. Kobayashi, Phys. Rev. A **70**, 023811 (2004).

[20] X. Yang, T. E. Dykstra, and G. D. Scholes, Phys. Rev. B **71**, 045203 (2005).

[21] A. Ruseckas and I. D. W. Samuel, Phys. Status Solidi C **3**, 263 (2006).

[22] A. Ruseckas, P. Wood, I. D. W. Samuel, G. R. Webster, W. J. Mitchell, P. L. Burn, and V. Sundström, Phys. Rev. B **72**, 115214 (2005).

[23] A. Shirakawa, I. Sakane, and T. Kobayashi, Opt. Lett. **23**, 1292 (1998).

[24] A. Shirakawa, I. Sakane, M. Takasaka, and T. Kobayashi, Appl. Phys. Lett. **74**, 2268 (1999).

[25] A. Baltuska, T. Fuji, and T. Kobayashi, Opt. Lett. **27**, 306 (2002).

[26] H. Kano, T. Santio, and T. Kobayashi, J. Phys. Chem. B **105**, 413 (2001).

[27] T. Kobayashi, Z. Wang, and T. Otsubo, J. Phys. Chem. A **111**, 12985 (2007).